SUPPLEMENTAL DATA

Supplemental Notes 1-4

Legends to Supplemental Figures 1-6 and Supplemental Tables 1, 2

SUPPLEMENTAL NOTES

Supplemental Note 1

Q-PCR and in situ hybridization experiments (examples in Supplemental Figure 3) as well as annotations in public databases together indicate that the retina made a major contribution to our datasets of genes exhibiting rhythmic expression in DD or LD in the eye (see Supplemental Tables 1 and 2, respectively). In the DD dataset, for example, genes with statistical ranks for rhythmicity in the top 100 out of 45,101 probe sets included a number with known expression exclusive to the retina or to neurons. Examples are *retinal s-antigen*, *phosphodiesterease 6b*, *phosphodiesterease 6g*, *syntaxin binding protein-1*, *trpC-1*, *trpM-1*, *recoverin*, *guanylate cyclase activator 1B*, *synaptic vesicle glycoprotein 2b*, *rims2, crx*, and *rgs-20*. The NetAffx Gene Ontology Mining Tool (http://www.Affymetrix.com), which allows objective consideration of the functions of genes in a given dataset, provided additional evidence of strong representation of genes expressed in the retina. For example, in the DD dataset (at a 15% false discovery rate), the two top-ranking Gene Ontology biological process terms for which associated genes were significantly over-represented in the dataset were “visual perception” and “neurophysiological process.” The dataset also included, as

expected, genes with expression limited to non-retinal ocular structures, such as *Lrat* (Supplemental Figure 3), *rpe65*, and *aquaporin-1.*

Chromatin re-modeling genes with robust rhythms of ocular expression in both DD and LD included Histone deacetylase 9; H3 histone, family 3B; MGC73635; Histone cluster 3, H2a; H2A histone family, member X; H1 histone family, member 0; Histone cluster 1, H1c.

For a graphical analysis of Gene Ontology biological processes represented in the DD and LD datasets, see Supplemental Figure 4.

Supplemental Note 2

Evidence for cyclic expression with a period of about one day in the microarrray expression datasets was measured using a standard *F*-statistic. Let $Y_1,\ldots,Y_{18}$ be the expression values for a particular probe set from arrays with corresponding time points $t_1,\ldots,t_{18}$. The relevant F-statistic compares the least-squares fits of the data under the null conditional mean model

$$E_0[Y_i|t_i] = \alpha_0 + \alpha_1 \sin(4\pi t_i/24) + \alpha 2 \cos(4\pi t_i/24) + \alpha 3 \cos(6\pi t_i/24) \quad (1)$$

and the alternative model

$$E_1[Y_i|t_i] = E_0[Y_i|t_i] + \alpha_4 \sin(2\pi t_i/24) + \alpha 5 \cos(2\pi t_i/24), \quad (2)$$

where $\alpha_0,\ldots,\alpha_5$ are scalar parameters. Taking (1) as the null model, rather than flat mean expression, makes the detection procedure specific for cyclic expression with a period of one day, since the null model accounts for cyclic expression with periods shorter than one day. The fitted models and the *F*-statistics can be computed using any basic statistical software package. P-values were assigned to each probe set by

comparing its observed F-statistic to the null distribution generated through 50,000 random permutations of its 18 time points. A list of genes with significant evidence for cyclic expression was obtained by controlling the false discovery rate (FDR) (Storey, J.D., Taylor, J.E., and Siegmund, D. [2004]. J. ROY. STAT. SOC. B *66*, 187-205).

Supplemental Note 3

Because of small differences in circadian period length in different mice, it is expected that in DD circadian oscillations of individual mice will drift slightly out of phase with respect to one another over the course of the three-day collection period, weakening the rhythmic signal in microarray analysis, which depends on synchronous population behavior. This effect could also be true for individual clock cells within a single eye if ocular clock cells are not strongly coupled. Therefore it is possible in principle that many more genes showed rhythmic expression in LD than DD because some fraction of the circadian rhythms of gene expression was too weak to detect in DD because of population desynchrony. In LD, entrainment of circadian oscillators results in perfect synchrony and therefore in very efficient detection of circadian rhythms (in addition to expression rhythms driven purely by LD cycles).

If significant desynchronization did in fact occur in DD over the three-day period, then it would necessarily have resulted in a systematic damping of amplitudes of the population expression rhythms over the three-day time-course. To assess this possibility, we performed inter-day correlation analysis of the 277 expression profiles defined as rhythmic in DD at a 15% false discovery rate. With no damping of amplitudes, correlation of the expression pattern from day-1 with that of day-3 should be

as good as the correlation of day-1 with day-2 (i.e., perfect repetition of waveforms and amplitudes). In this case, a plot of the day-2 : day-1 correlation against the day-3 : day-1 correlation would be expected to fall on the diagonal, with variance symmetrically distributed about the diagonal, indicating no systematic loss of fidelity of the expression rhythm over time. In contrast, a systematic damping of amplitudes would result in a substantial shift of points to the right side of the diagonal (reflecting a relative degradation of the population rhythm on day-3). Supplemental Figure 4A shows a plot of the inter-day correlations of the rhythmic expression profiles in DD. There is a roughly symmetrical distribution about the diagonal, with a small preponderance of points falling to the right of the diagonal (59%) compared to the left (41%). This result suggests a broad but rather mild dampening of amplitudes. Consistent with inspection of individual rhythmic profiles, which show only occasional damping of amplitude, the analysis suggests that there was only a modest degree of population desynchronization over the three-day period in DD.

If this mild decay of rhythmic fidelity in DD led to a substantial underestimate of genes with rhythmic expression patterns in DD compared to LD, then genes classified as rhythmic in LD but not in DD should show a tendency toward high, sub-threshold rankings for rhythmicity in DD. To test this hypothesis, we selected the 2449 genes with rhythmic expression in LD (at a 15% false discovery rate) that were not classified as rhythmic at the same threshold in DD. These genes all had rhythmicity rankings in LD in the top 2,670 out of 30,923 probe sets (14,178 probe sets with unreliable signals were excluded from analysis; see Experimental Procedures). If a substantial proportion of these genes did in fact have rhythmic expression in DD that was misclassified

because of damping or noise, then a plot of rank for rhythmicity in LD of these genes against rank for rhythmicity in DD should show a systematic bias towards higher rankings in DD (even though they were below threshold in DD). Instead, the plot shows that the DD rankings of the genes are widely distributed across the full range (1-30,923), with only very few clustered at high rankings (Supplemental Figure 4B). Thus most of the genes show no evidence of subthreshold rhythmic expression in DD. This result suggests that the number of genes with rhythmic profiles in DD was likely underestimated to some extent, but that a large majority of genes with rhythmic expression in LD are driven by the LD cycle and not by the circadian clock.

Supplemental Note 4

To detect evidence of cyclic expression in the one-day, six-array datasets from wildtype and *Bmal1*$^{-/-}$ mice, we tested for a significant Pearson correlation between expression values in the six arrays and the corresponding estimated expression values from the LD data set. These tests of correlation were only carried out for genes that were first selected as cycling in LD at 15% FDR in the three-day dataset. To assess the significance of correlation, each probe set's correlation coefficient was compared to the distribution of correlation coefficients one would expect if the one-day data represented independent Gaussian noise. This null distribution was used to assign a P-value to each probe set. Sets of genes with significant evidence for cyclic expression in the six-array data set were then obtained by controlling the FDR (Storey, J.D., Taylor, J.E., and Siegmund, D. [2004]. J. Roy. Stat. Soc. *B 66*, 187-205).

LEGENDS TO SUPPLEMENTAL FIGURES 1-6 AND SUPPLEMENTAL TABLES 1-2

Supplemental Figure 1 Likely circadian clock cells in the mammalian inner retina

(A) Mouse retina sections showing nuclear immunofluorescence staining for clock components CLOCK (green), PER1 (green), or PER2 (green) and Tyrosine Hydoxylase (TH; red) to mark dopaminergic amacrine cells, as indicated. The very faint fluorescent band at top of images represents common non-specific staining of the retinal pigment epithelium. Immunostaining was carried out as described (Gustincich et al. [1999]. J. Neurosci. *19*, 7812-22.) using rabbit polyclonal antibodies against PER1, PER2, and CLOCK (Alpha Diagnostics) at a dilution of 1:250 and anti-TH mouse monoclonal antibody (ImmunoStar) at 1:1000. (B) Mouse retina sections showing in situ hybridization for mRNAs encoding various clock-related proteins, as indicated. The hybridization signal is a dark purple-black stain; the pinkish coloration is non-specific labeling of layered retinal structures. Sense control riboprobes showed no specific labeling (not shown). Tissues were harvested at the expected times of peak expression for the indicated proteins or transcripts: CLOCK, PER1, PER2: CT12.5; *Per1*, *Per2*, *Per3*, *Dbp*: CT8.5; *Rev-erb*α: CT4.5. PL, photoreceptor layer; INL, inner nuclear layer; GCL, ganglion cell layer.

Supplemental Figure 2 Summary of microarray experiment to identify genes with 24-hour rhythms of expression in the mouse eye

(A) Scheme of three-day collection of mouse eyes. 108 male CBA/CaJ mice were entrained for three weeks in a 12:12 light-dark cycle (LD), then split into two equal groups during the dark phase, one remaining in LD and the other transferred to constant darkness (DD). Whole eyes were collected at four-hour intervals (six eyes from three mice per time-point) over three days for each condition (collection times are indicated by "X"). White and black bars respectively represent light or darkness. Collections in darkness were performed under infrared illumination with binocular night vision goggles. (B) Summary of algorithm used to detect circadian and diurnal rhythms of gene expression from microarray data.

Supplemental Figure 3 Circadian gene expression rhythms detected by microarray can be assigned to specific ocular structures by quantitative PCR

(A-D) Top, circadian expression profiles determined by Q-PCR (average of N = 3) from three dissected eye fractions, retina, lens, and the remainder (E-R,L), as indicated. Each of the fractions of the eye accounts for approximately 1/3 of total eye RNA, and equal aliquots of RNA from each source were used for the assays. Bottom, confirmation of the cellular source of circadian rhythm of each transcript by in situ hybridization, performed on retinas collected at times corresponding to the maximum and minimum expression for each transcript. To visualize a signal in the retinal pigment epithelium (RPE), in situ hybridization for *Lrat* was performed on retinal sections from albino C57BL/6 mice. *Dbp*, D-site albumin promoter binding protein; *L-rat*, lecithin-retinol acyltransferase; *Drd4*, D4 dopamine receptor. (E) Potential circadian intercellular signals in the retina**.** In situ hybridization to mouse retina sections showing localization

of the indicated rhythmic transcripts (at the approximate time of peak expression) encoding secreted factors (*Il-18*: CT0.; *Ctgf*: CT12.5). Localization is consistent with expression in circadian clock cells (Supplemental Figure 1). *Il-18*, interleukin-18; *Ctgf*, connective tissue growth factor.

Supplemental Figure 4 Global representation of the biological processes associated with genes exhibiting daily rhythms of expression in the mouse eye in constant darkness (DD) or in a 12h-12h light-dark cycle (LD). Each tree (gray dots and connecting paths) represents categories (dots) in the Gene Ontology (GO) hierarchy for biological process that matched 60 or more of the 24,718 probe sets classified as expressed in DD or the 24,884 classified as expressed in LD, which respectively comprised 7,908 and 7,952 unique genes associated with one or more GO terms. Superimposed on each respective tree (in red) are the biological processes that matched 5 or more of the 120 genes stringently classified as rhythmic in DD or that matched 20 or more of the 1032 genes stringently classified as rhythmic in LD (both at 5% false discovery rate). In DD and LD, the rhythmically-expressed gene sets mapped to multiple high-level categories, as indicated, and extended across the full width of the tree, indicating association with a broad range of biological processes. The parameters were selected to produce a clear graphical display; results were similar across a wide range of parameter values both for tree resolution and for selection of rhythmically-expressed genes (not shown). Each tree shows more than 400 biological process categories. For inclusion in the set of expressed genes that generated the gray backbone of the tree, a probe set had to satisfy the “expressed” criterion

(http://www.Affymetrix.com/products/algorithms_tech.htm) on at least 10 of the 18 arrays. GO biological process trees were created as described (Zhong S., Storch K.F., Lipan O., Kao M.C., Weitz C.J., and Wong W.H. [2004] Appl. Bioinformatics *3*, 261-264; http://www.GoSurfer.org).

Supplemental Figure 5 Damping of amplitudes in DD is unlikely to account for the large excess of genes showing rhythmic expression in LD as compared to DD (see Supplemental Note 3 for discussion).

(A) For the 277 expression profiles defined as rhythmic in DD at a 15% false discovery rate (in the three-day experiment in Figure 1), the correlation between day-2 and day-1 was plotted against the correlation between day-3 and day-1. A systematic loss of amplitude over the three-day period would result in a substantial shift of points to the right of the diagonal, reflecting a relatively degraded rhythmic profile on day-3. The small majority of points to the right (59%) indicates a small but significant degradation of the rhythmic signal over the three-day period. (B) For each of the 2449 genes with rhythmic expression in LD (at a 15% false discovery rate) that were not identified as rhythmic in DD at the same threshold, the rank for rhythmicity in LD (all of the genes ranked above 2670 out of 30,923) was plotted against the rank in DD. The wide distribution of ranks in DD (across the full range of 1-30,923) indicates that strong rhythmic expression in LD is not in general correlated with a sub-threshold tendency toward rhythmicity in DD. The small cluster with relatively high ranking in DD at the lower left likely represents a subset of genes with weak rhythms in DD. The result suggests that the number of genes with rhythmic expression in DD was underestimated

to a modest extent, but that this underestimate can account for only a small fraction of genes showing rhythmic expression in LD.

Supplemental Figure 6 *Bmal1* and retinal circadian rhythms

(A) *Bmal1* is required for circadian molecular rhythms in the mouse eye, as expected. Circadian expression profiles (in DD) of the indicated transcripts from eyes were determined by Q-PCR for wildtype mice and *Bmal1*$^{-/-}$ littermates, as indicated. Shown are the mean and SEM (N = 3). (B) Two general molecular defects of circadian physiology in the absence of *Bmal1*. Diagram represents the CLOCK-BMAL1 heterodimeric transcription factor (labeled open boxes) bound to its recognition site on genomic DNA (closed box on horizontal line). Red "X"'s indicate defects in the absence of a functional *Bmal1* gene. **Left**, Transcriptional activation (plus sign) of genes encoding proteins involved in the circadian negative feedback loop that inhibits CLOCK-BMAL1 function (dashed curve; minus sign), such as *Per1* and *Per2*. Absence of *Bmal1* function abolishes circadian rhythmicity by abolishing the circadian feedback loop. **Right**, Transcriptional activation (plus sign) of genes encoding proteins not involved in clock function but which serve as direct outputs of CLOCK-BMAL1 activity (transcriptional outputs). Absence of *Bmal1* function is expected to reduce transcriptional activation of those output pathways directly driven by CLOCK-BMAL1 approximately to their trough levels.

Supplemental Table 1 Genes exhibiting circadian rhythms of expression in the mouse eye in constant darkness (DD) at a threshold corresponding to a 15% false discovery rate

Genes are ordered by their quantitative ranking for strength of rhythmicity in constant darkness (DD. Column at left indicates the Affymetrix probe set identifier. For comparison, the rank for strength of rhythmicity in a light-dark cycle (LD) is also shown. Column marked “Phase (CT)” indicates the phase of peak expression in circadian time. Gene Ontology Biological Process terms associated with each gene are listed in the two columns at right. #, Genes for which three-day expression profiles were assessed by quantitative RT-PCR.

Supplemental Table 2 Genes exhibiting diurnal rhythms of expression in the mouse eye in a light-dark cycle (LD) at a threshold corresponding to a 5% false discovery rate

Genes are ordered by their quantitative ranking for strength of rhythmicity in a light-dark cycle (LD). Column at left indicates the Affymetrix probe set identifier. For comparison, the rank for strength of rhythmicity in constant darkness (DD) is also shown**.** Column marked **“**Phase (ZT)” indicates the phase of peak expression in Zeitgeber time. Gene Ontology Biological Process terms associated with each gene are listed in the two columns at right. #, Genes for which three-day expression profiles were assessed by quantitative RT-PCR. ##, Genes for which one-day expression profiles in wildtype and *Bmal1*$^{-/-}$ mice were assessed by quantitative RT-PCR.

[F] Supp. Figure 1

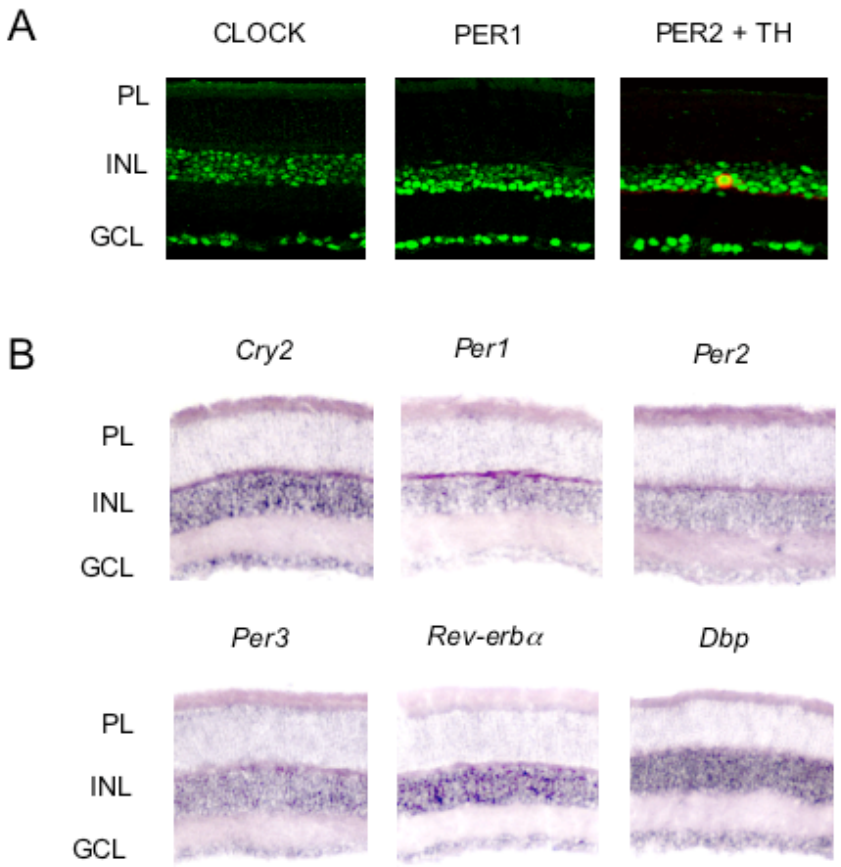

Supplemental Fig. 1

[F] Supp. Figure 2

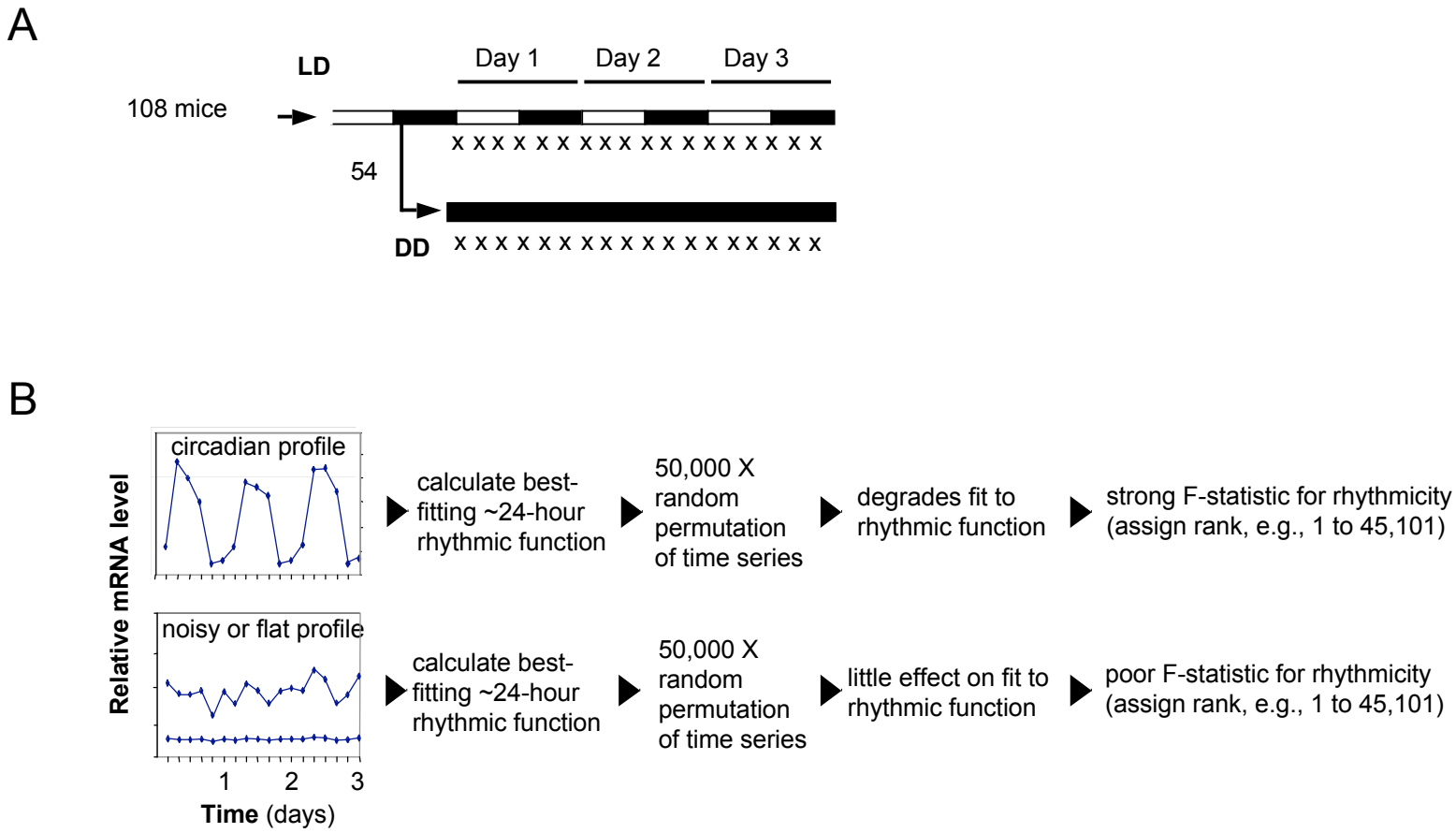

Supplemental Fig. 2

[F] Supp. Figure 3

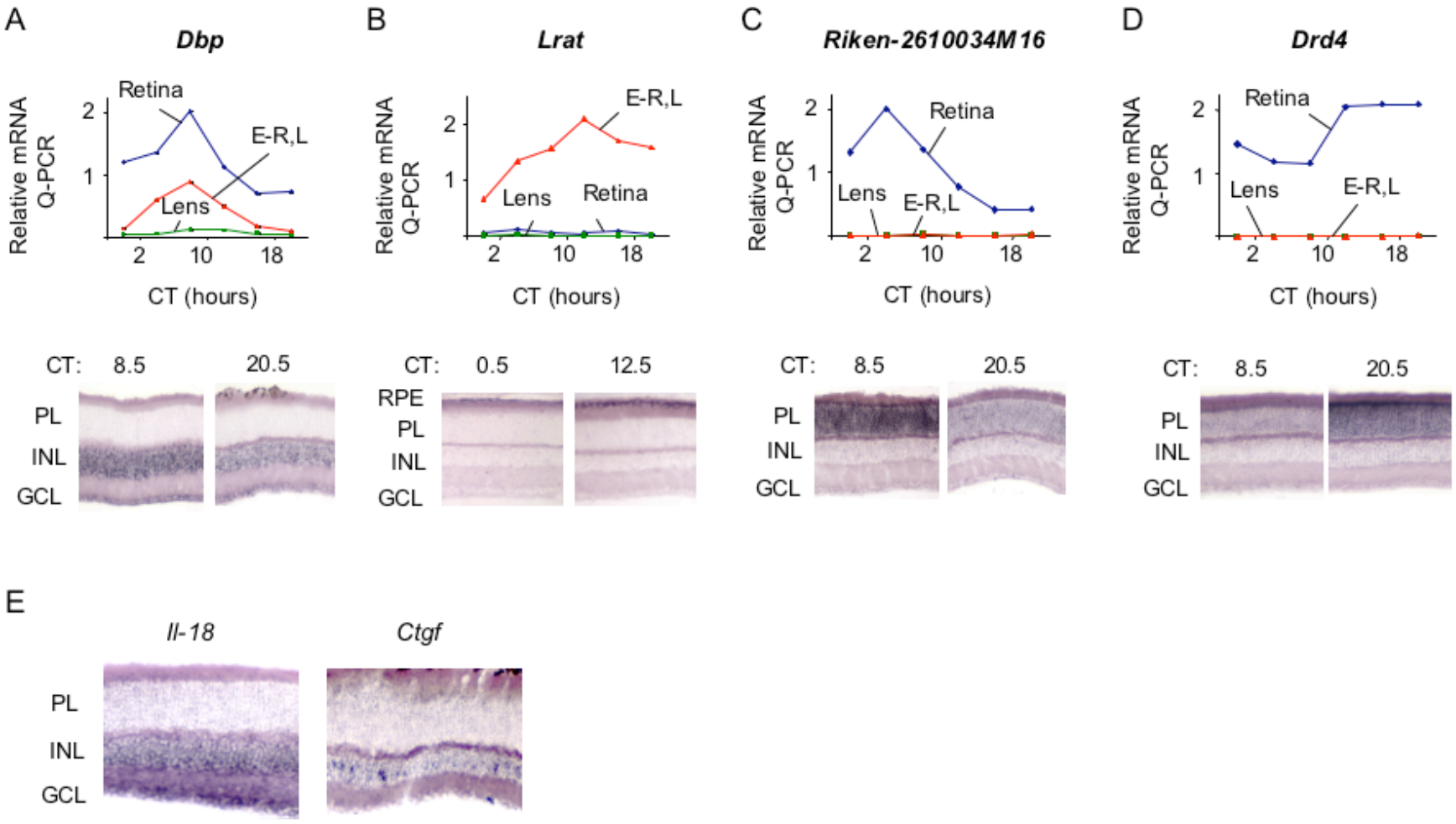

Supplemental Fig. 3

[F] Supp. Figure 4

DD

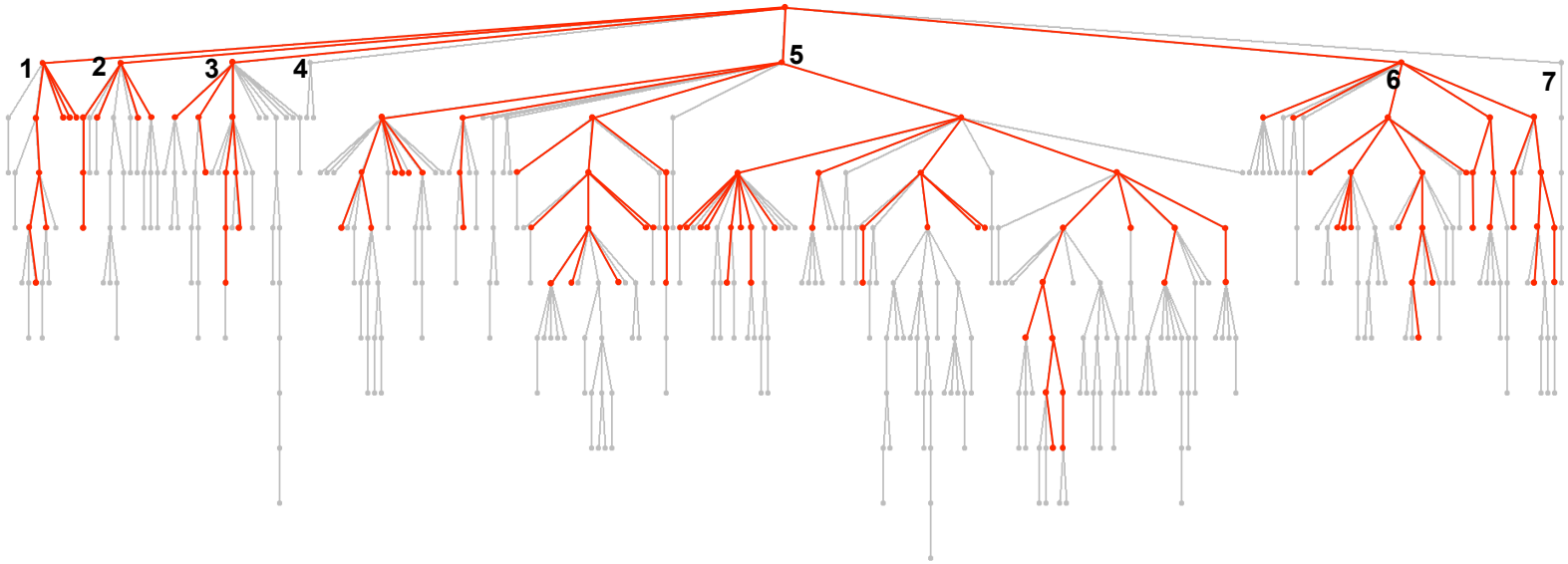

LD

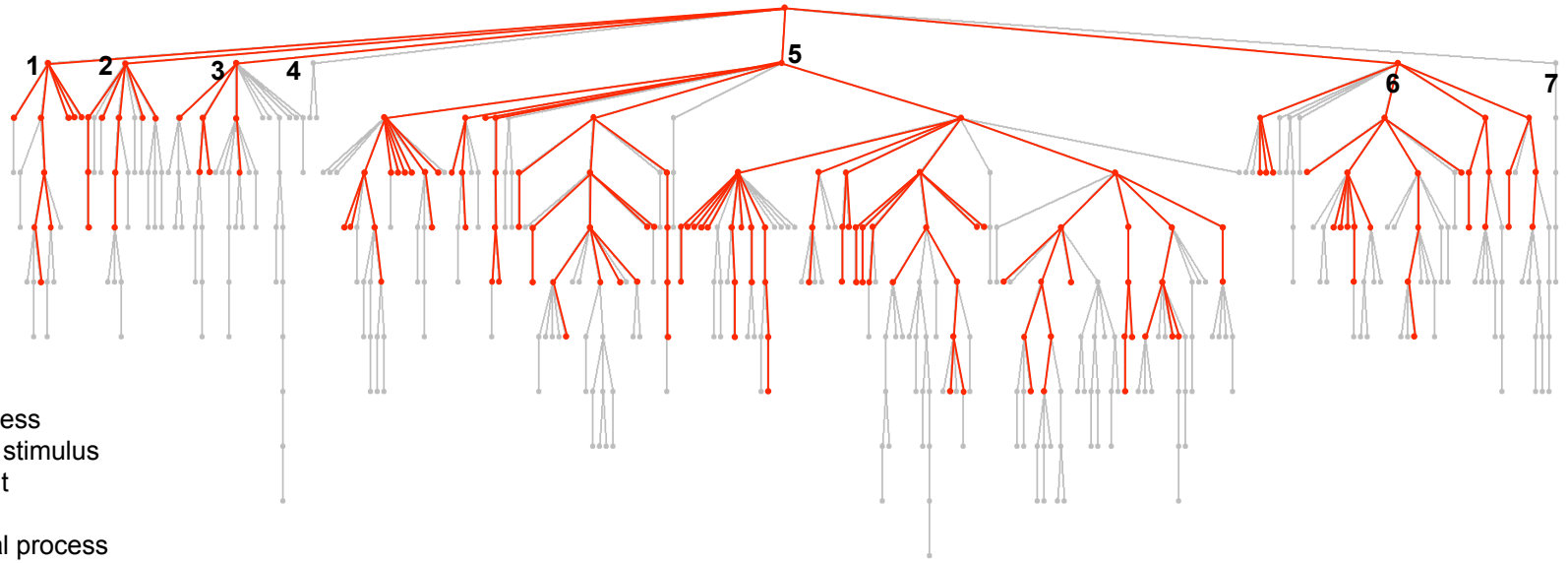

1 cellular process
2 response to stimulus
3 development
4 growth
5 physiological process
6 regulation of biological process
7 reproduction

Supplemental Fig. 4

[F] Supp. Figure 5

A

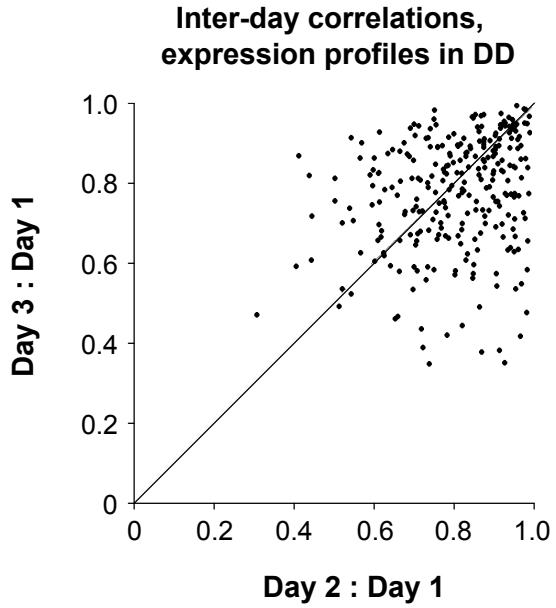

B

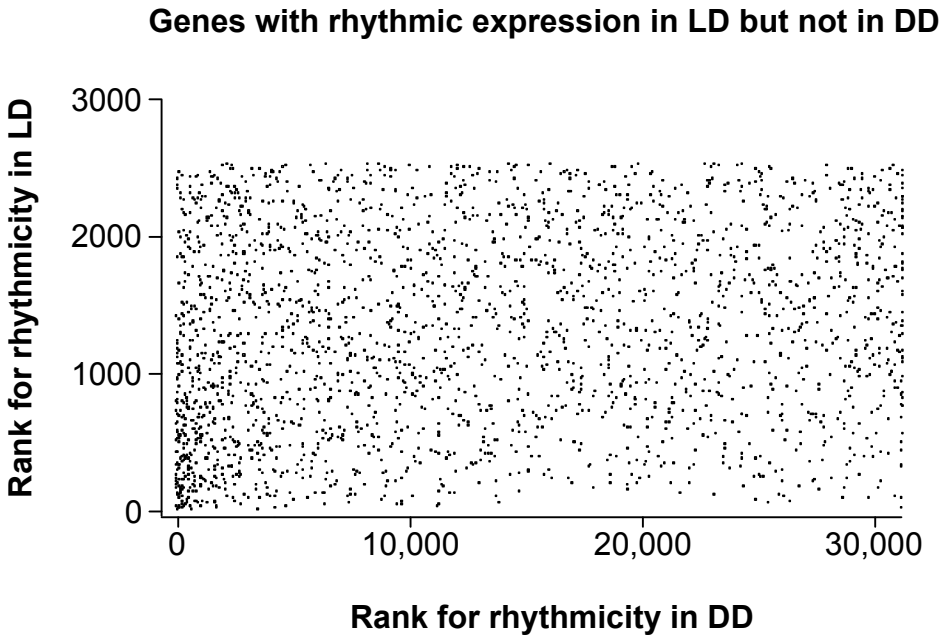

Supplemental Fig. 5

[F] Supp. Figure 6

A

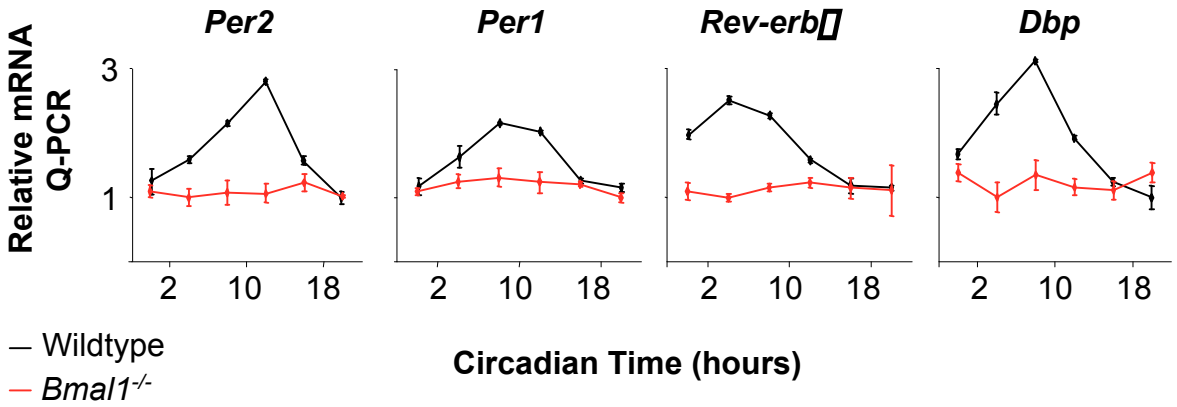

B

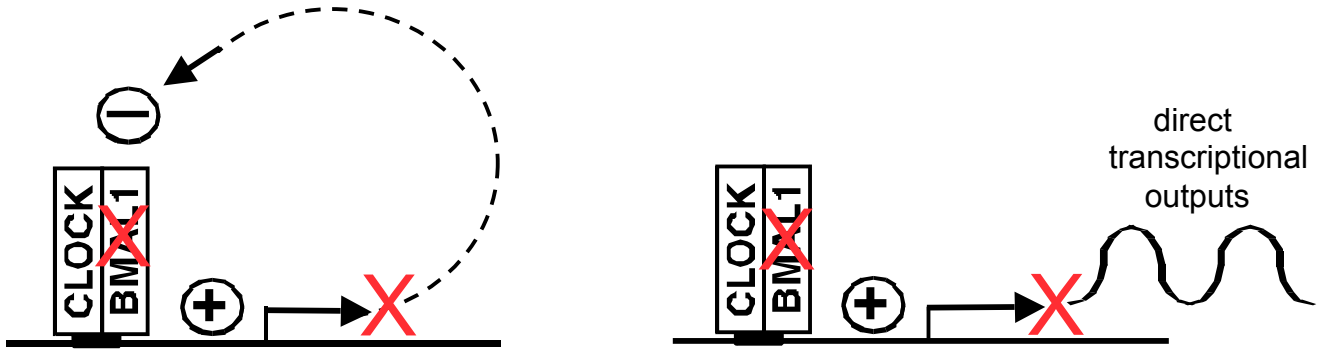

Supplemental Fig. 6